



ISSN 1335-8871

MEASUREMENT SCIENCE REVIEW

Journal homepage: <https://content.sciendo.com>

New Measurement Method of Oil-Water Two-Phase Flow with High Water Holdup and Low Rate by Phase State Regulation

Lianfu Han^{1,2}, Ming Chen², Xingbin Liu², Changfeng Fu^{3*}

¹*School of Electrical and Automation Engineering, Changshu Institute of Technology, South Third Ring Road, No.99, 215500, Suzhou, China, lianfuhan@nepu.edu.cn*

²*School of Physics and Electronics Engineering, Northeast Petroleum University, Xuefu Street Road, No99, 163318, Daqing, China, chenming@stu.cqu.edu.cn*

³*School of Electronic and Information Engineering, Changshu Institute of Technology, South Third Ring Road, No.99, 215500, Suzhou, China, changfengfu@nepu.edu.cn*

Abstract: Flow rate and holdup are two essential parameters to describe oil-water two-phase flow. The distribution of oil-water two-phase flow in the pipeline is very uneven, and there is a significant slippage between the phases. This makes it difficult to measure these two flow parameters. In this paper, a new measurement method of flow rate and holdup based on phase state regulation is proposed. The oil-water two-phase flow is adjusted to oil or water single-phase flow according to the time sequence by the phase state regulation, and the oil-water phase interface is measured with a conductance sensor. A wavelet transform based phase inflection point detection model is proposed to detect the oil-water phase change point. The experimental results show that the maximum measurement error of the flow rate of water is 3.73%, the maximum measurement error of the flow rate of oil is 3.68%, and the flow rate measurement repeatability is 0.0002. The accuracy of the measurement holdup is better than 3.23%, and the repeatability of the measurement holdup is 0.0003. The prototype designed based on this method has two advantages. One is that it is small in size, the other is that it does not depend on the accuracy of the sensor. Therefore, it can be widely used in oilfield ground measurement.

Keywords: Oil-water two-phase flow, phase state regulation, flow rate, holdup.

1. INTRODUCTION

After the oilfield enters the middle and late stages of development, water holdup increases and crude oil production decreases [1]. For example, in one block of the Daqing Oilfield there are about 23800 oil wells. The average liquid production of a single well is less than 15 m³/d, and the average water holdup is 98.6%. Due to the complex and variable flow patterns of oil-water two-phase flow [2], the distribution of oil and water in the pipeline is extremely uneven. There is significant oil-water inter-phase slippage, and measurement parameters such as total flow rate and phase holdup are coupled. This makes it very difficult to measure the oil-water two-phase flow parameters. The interpretation of logging data and the accuracy of logging instruments largely depend on the flow rate and holdup parameters [3]-[5]. Therefore, flow rate and holdup are two essential parameters to describe the oil-water two-phase flow.

The measurement of flow rate and holdup is divided into a separation method and a non-separation method. The non-separation methods mainly include the turbine method [6]-[11], the ultrasonic method [12], [13], the correlation method

[14], the tracer method [15], the electromagnetic method [16], [17] and the microwave method [18], [19]. The above non-separation methods have good measurement results in some fields. However, they still have shortcomings in flow rate and holdup measurement of high-water holdup and low-rate oil-water two-phase flow with low flow rate. The main drawback of the turbine method is that the response characteristics of the turbine flow sensor are significantly affected by the well inclination angle and the fluid viscosity [20]. The disadvantage of the ultrasonic method is that its theoretical model needs further improvement [21]. The correlation flow method requires two sets of sensors and cannot meet the volume limit of the narrow measurement space [22]. The tracer method [23] is divided into particle tracers, thermal tracers and radioactive tracers [24], [25]. Radioactive tracer is divided into the radioactive isotope tracer method and the pulsed neutron-oxygen activation method [26], [27]. The disadvantage of the radioactive isotope tracer method is that the use of radioactive sources does not meet the safety and environmental protection requirements. The disadvantages of the pulse neutron oxygen activation method are the high

instrument costs and the short lifetime of the neutron tube. The electromagnetic method has yet to be studied for high water holdup and low-rate oil-water two-phase flow [28]. Separation methods mainly include the partial separation method [29], [30] and the full separation method [31], [32]. In the partial separation method, the equipment volume is significantly reduced. However, the high-speed rotation in the cyclone causes droplet break. This makes oil-water separation difficult. Therefore, the measurement accuracy of the partial separation method is limited. The full separation method not only completely solves the problem of parameter coupling, but also has the advantages of high measurement accuracy and a wide measurement range. In addition, it is not affected by flow pattern change. However, the equipment volume using the full separation method is always very large.

In the existing oil-water two-phase flow measurement methods, the equipment volume using the separation method is too large. The non-separation methods often directly use sensors to measure flow and holdup. The measurement accuracy of non-separation methods is highly dependent on the accuracy of the sensor. To solve these problems, this paper proposes a new flow rate and holdup measurement method based on phase state regulation. In the measurement method proposed in this paper, the oil-water two-phase flow is adjusted to oil phase flow and water single flow in chronological order by phase state regulation. The sensor used in this method only detects the oil-water interface. Therefore, a high measurement accuracy of the flow can be achieved.

2. MEASUREMENT PRINCIPLE

A. Measurement method of oil-water two-phase flow

The measurement principle is as follows: By regulating valves 1, 2 and 3, the oil-water two-phase flow from the inlet becomes a single-phase flow of oil or water, which flows in time sequence when it reaches the conductance sensor. The oil phase or the water phase are judged by the signal from the conductance sensor. Then the flow rate and holdup are calculated according to the volume of the measurement tank and the accumulated time.

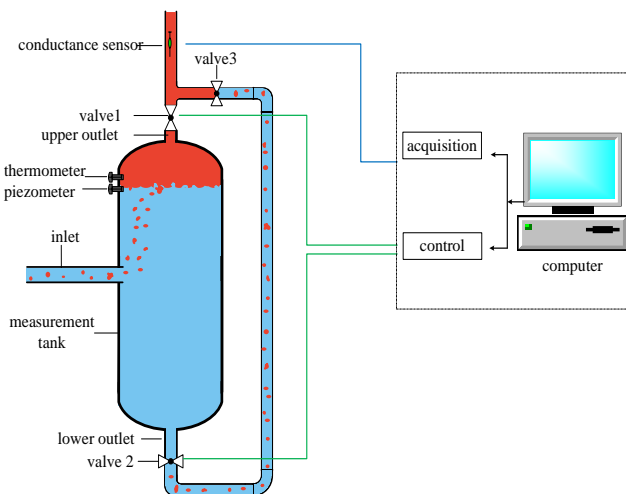


Fig. 1. Diagram of measurement principle.

As shown in Fig. 1, first, the oil-water two-phase flow enters the measurement tank from through inlet; then the oil-water two-phase flow in the measurement tank is regulated into oil layer and water layer by gravity; then the measurement tank is filled with the oil layer and water layer; then the oil layer and water layer are regulated at the outlet into single-phase oil, oil-water two-phase and single-phase water by regulating the valves. At last, the sensor detects the phase state, and the accumulated time is recorded. The flow rate and holdup of the oil-water two-phase flow are determined by the accumulated time. The detailed measurement process is as follows:

Measurement of flow rate

The measurement tank is initially empty. The signal level of conductance sensor in Fig. 2 is low. Open valves 2, 3 and close valve 1 so that the oil-water two-phase flow enters the measurement tank through the inlet. At the same time, the timer starts to record time. The beginning time is called 0. The oil-water two-phase flow in the measurement tank is regulated into an oil layer and a water layer by gravity. When the measurement tank is filled with the flow, the water layer flows out of the measurement tank through the lower outlet and the oil layer continues to accumulate. At this time, the conductance sensor signal level goes from a low level to a high level (at point A). When the oil layer reaches the conductance sensor, the signal level of the conductance sensor goes from a high level to a low level (at point B). The flow rate of oil v_o is expressed by (1):

$$v_o = \frac{V + \Delta v}{t_B} \tag{1}$$

where V is the volume of the measurement tank, Δv is the volume of the pipe from the lower outlet to valve 3, and t_B is the time when the signal level of the conductance sensor goes from high level to low level.

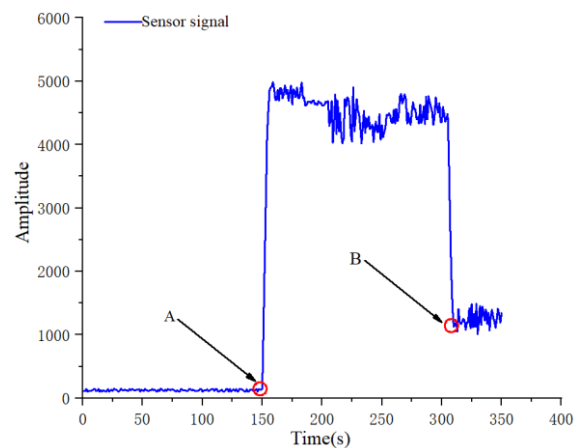


Fig. 2. Diagram of the conductance sensor signal.

According to (1), the oil flow rate is achieved. Similarly, the water flow rate v_w is achieved as (2):

$$v_w = \frac{V}{t_w} \tag{2}$$

where t_w is the water accumulation time.

Measurement of holdup

The measurement equipment volume has a fixed size. Therefore, the holdup of oil or water is inversely proportional to their accumulation time. Considering the volume difference between the oil phase measurement and the water phase measurement, the water holdup h_w and the oil holdup h_o are calculated by (3):

$$\begin{cases} h_o = \frac{t_w \times (\frac{V+\Delta v}{V})}{t_B + t_w (\frac{V+\Delta v}{V})} \\ h_w = \frac{t_B}{t_B + t_w (\frac{V+\Delta v}{V})} \end{cases} \quad (3)$$

B. Recognition of oil-water two-phase flow phase change point

As shown in Fig. 2, the signal amplitude of the oil-water two-phase flow changes abruptly when the conductance sensor has detected the phase change point of the oil-water two-phase flow. The detection of the phase change point of the oil-water two-phase flow belongs to the determination of the signal singularity. According to the signal singularity, the wavelet coefficient modulus maxima method is used to detect the mutation point of the signal on the appropriate scale. In this paper, the wavelet analysis method is used to detect the critical point of the oil-water signal.

The wavelet function is divided into two classes. When the wavelet function is the first derivative of the smoothing function, the local extremum of the modulus is considered as a signal mutation point. When the wavelet function is the second derivative of the smoothing function, the zero-crossing point of the modulus is considered as the signal mutation point. Therefore, the zero-crossing point of the modulus of the wavelet transform coefficient and the local extremum point are used to detect the signal mutation point.

The modulus maxima mutation detection procedure is as follows: First, the signal is smoothed; finally, the mutation point is detected using the first and second derivatives of the smoothed signal. $\theta(x)$ is a smooth function, which satisfies $\int_{-\infty}^{+\infty} \theta(x) dx = 1$. $\psi^1(x)$ and $\psi^2(x)$ are the first and second derivatives of $\theta(x)$, respectively. They satisfy the following admissible conditions:

$$\int_{-\infty}^{+\infty} \psi(x) dx = \int_{-\infty}^{+\infty} \frac{d\theta(x)}{dx} dx = 0 \quad (4)$$

Therefore, $\psi^1(x)$ and $\psi^2(x)$ are all wavelets. We can obtain the wavelet transform of the function $f(x)$ over wavelet $\psi^1(x)$ and $\psi^2(x)$ on scale j and position x :

$$\begin{cases} W_2^1 j f(x) = f \cdot \psi_j^1(x) = j \frac{d}{dx} (f \cdot \theta_j)(x) \\ W_2^2 j f(x) = f \cdot \psi_j^2(x) = j^2 \frac{d^2 \theta_j}{dx^2} \frac{d^2}{dx^2} (f \cdot \theta_j)(x) \end{cases} \quad (5)$$

The wavelet transform is obtained from the convolution of the function $f(x)$ and the smooth function θ_j multiplied by j and j^2 with respect to the first and second derivatives of j . The local extremum of $W_2^1 j f(x)$ corresponds to the zero-crossing point of $W_2^2 j f(x)$ and the inflection point of $f \cdot q_j(x)$.

Multi-scale detection can determine the exact location of the mutation point. Multi-scale mutation point detection serves to smooth the function $f(x)$ through the smooth function $\theta_j(x)$ corresponding to scale j and it is expressed as $f \cdot q_j(x)$. When the scale j is small, the steep mutation part of $f(x)$ is preserved; when the scale j is large, some characteristics of the large-scale slow change are preserved, which are erased by the filtering effect. The scale factor j can properly adjust the parameter values according to the characteristics of $f(x)$, and then effectively detect the positions of the different mutation points of $f(x)$ in the signal. Therefore, the mutation points on different scales are determined by different j values.

3. DESIGN AND OPTIMIZATION OF EXPERIMENTAL PROTOTYPE

To study the influence of the measurement tank geometric structure on the measurement, two-dimensional simulation is used to simulate the flow pattern in the measurement tank. The volume, shape, internal structure, size and position of the inlet are analyzed one by one. Then, the influence of the flow rate change on the results is simulated to further optimize the measurement tank and determine the final scheme for its simulation.

The initial parameters of the prototype are shown in Fig. 3. The application conditions of the experiment are as follows: the upper limits for the water and oil phase flow rates are 10.00 m³/d and 30.00 m³/d, respectively; the pressure upper limit is 3.00 MPa; the temperature range is 40.00 °C-100.00 °C.

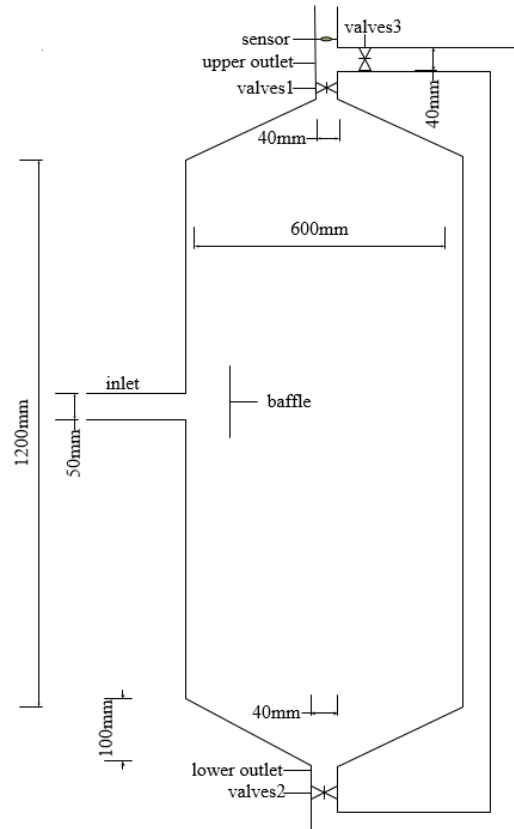


Fig. 3. Intention of prototype structure.

The simulation nephogram and the dynamic curve of the oil phase detected at the sensor position are shown in Fig. 4. As shown in Fig. 4, for a total inlet flow rate of 40.00 m³/d, the cross-sectional velocity is 0.26 m/s and the Reynolds number and turbulence intensity are 10606.02 and 0.05, respectively. The oil-water interface is clear and the scheme is reasonable.

According to the simulation results, the final prototype parameters are as follows: the inner diameter of the inlet is set to 50.00 mm and a baffle with a height of 100.00 mm is placed vertically 50.00 mm away from the inlet. The inner diameter of the upper and lower outlet is 40.00 mm, the height of the measurement tank is 1200.00 mm and the inner diameter is 600.00 mm. The upper and lower ends of the tank are conical and have a height of 100.00 mm.

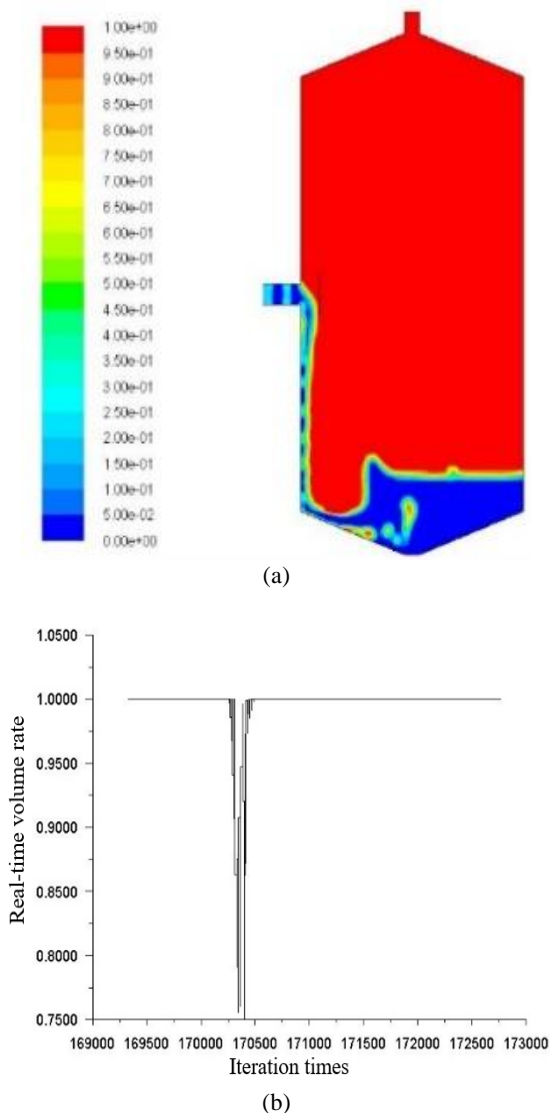


Fig. 4. The simulation nephogram and dynamic curve of oil phase (a) simulation nephogram; (b) dynamic curve.

4. EXPERIMENT

To verify the flow rate and holdup measurement method of the oil-water two-phase flow with a low flow rate proposed in this paper, an experimental prototype was created, as shown in Fig. 5.

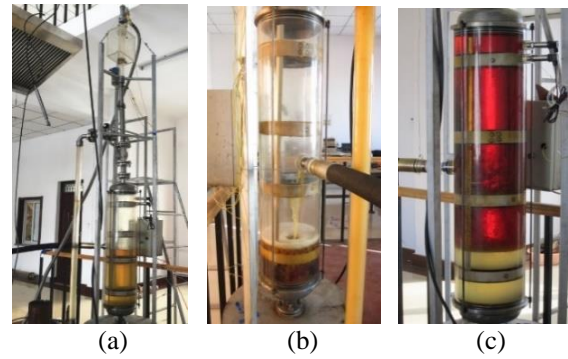


Fig. 5. Diagram of the experimental system: (a) system device; (b) measurement of water; (c) measurement of oil.

The experimental prototype consists of a conductance sensor array for export flow pattern identification, a collection, control and export flow pattern identification module and a measurement tank. The measurement tank contains an inlet distributor, a flow field buffer component, three shutter valves and a temperature sensor. The measurement tank is made of acrylic PMMA. The temperature sensor is a Pt100 temperature sensor and the output signal is a 4 mA ~ 20 mA DC signal. The inner diameter of the transmission pipe is 40.00 mm and the wall thickness is 5.00 mm. The transmission pipe is made of PMMA, and the DN50 flange is used to connect with the oil well. Three shutter valves adopt a hydraulic valve, and turn off time is 0.10 s. The conductance sensors are equipped with six-electrode conductance sensors.

The oil-water holdup and flow rate are controlled by the multiphase flow control system, and the oil-water two-phase flow flows into the measurement tank after full stabilization. The experimental parameters are as follows:

- temperature: 20.00 °C;
- pressure: 100.00 KPa;
- flow rate of oil: 0-30 m³/d;
- flow rate of water: 0-30 m³/d;
- water holdup: 30%-70%;
- length of steady flow section: 2000.00 mm;
- Δv : 0.0019 m³.

5. RESULTS AND DISCUSSION

A. Oil-water two-phase flow measurement experiment

Many measurement experiments are performed. One array of measured data is shown in Fig. 6. The data are processed by the recognition method of oil-water two-phase flow phase change point, and the phase change point is shown in Fig. 6. In Fig. 6, the water phase accumulation time is 659.00 s and the oil phase accumulation time is 337.00 s by the phase change point detection method of oil-water two-phase flow. The actual flow rate of oil is 5.00 m³/d and the actual flow rate of water is 10.00 m³/d. The measurement value of the flow rate of oil is 4.93 m³/d and the measurement value of the flow rate of water is 10.20 m³/d. Thus, the measurement error for the flow rate of oil is 1.22% and the measurement error for the flow rate of water is 3.03%. The actual oil holdup is 33.33% and the actual water holdup is 66.67%. Therefore, the measured oil holdup is 33.90%, the measured water holdup is 67.21% and the measurement error for water is 2.35%.

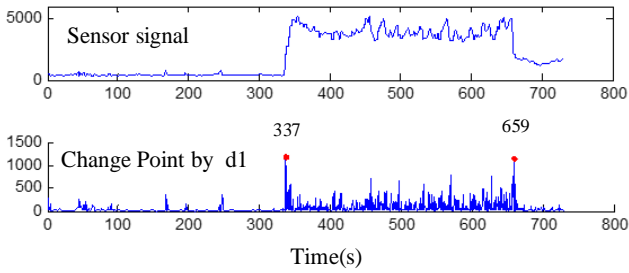


Fig. 6. The results of the measurement experiment.

B. Repeatability of the oil-water two-phase flow measurement experiment

To reduce the measurement uncertainty, many experiments are performed with different flow rates and different holdups. The experimental results are shown in Fig. 7 and Fig. 8. In Fig. 7 and Fig. 8, each measurement value is the average of 30 measurement values.

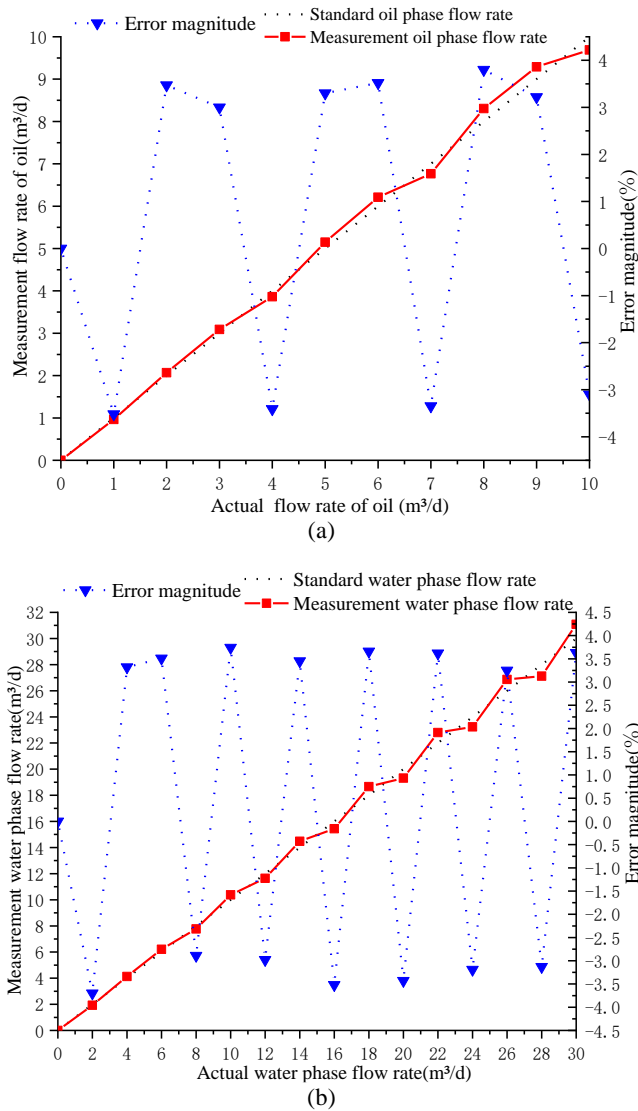


Fig. 7. Experimental diagram of randomness of the oil-water two-phase flow measurement: (a) oil measurement, (b) water phase measurement.

As shown in Fig. 7, the average error of the flow rate measurements of oil is 3.37%. The maximum error is 3.68% when the actual flow rate is 8.00 m³/d. The minimum error is 3.00% when the actual flow rate is 3.00 m³/d. Therefore, the flow rate of the oil measurement accuracy is better than 3.68%.

The average error of the flow rate measurements of water is 3.40%. The maximum error is 3.73% when the actual flow rate is 2.00 m³/d. The minimum error is 2.89% when the actual flow rate is 12.00 m³/d. Therefore, the flow rate of the water measurement accuracy is better than 3.73%.

For a flow rate of oil measurement from 1 m³/d to 10 m³/d, the mean square error is 0.0022, 0.0031, 0.0024, 0.0021, 0.0019, 0.0023, 0.0017, 0.0025, 0.0028 and 0.0026, and the repeatability is less than 0.0002.

For a flow rate of water measurement from 1 m³/d to 30 m³/d, the mean square error is 0.0019, 0.0024, 0.0033, 0.0037, 0.0023, 0.0029, 0.0017, 0.0026, 0.0028, 0.0029, 0.0026, 0.0031, 0.0027, 0.0022 and 0.0024, and the repeatability is less than 0.0002.

In Fig. 8, the average error of the measurement experiment of water holdup is 2.84%. The maximum error is 3.23% when the actual holdup is 25.00%. The minimum error is 2.10% when the actual holdup is 50.00%. Therefore, the accuracy of the holdup measurement is better than 3.20%. For a flow holdup measurement from 30% to 70%, the mean square error is 0.0023, 0.0029, 0.0034, 0.0021, 0.0025, 0.0026, 0.00017, 0.0025, 0.0028, 0.0024, 0.0029, 0.0027, 0.0029, 0.0028, 0.0032, 0.0023, 0.0035, 0.0026, 0.0031, 0.0025 and 0.0032, and the repeatability is less than 0.0003.

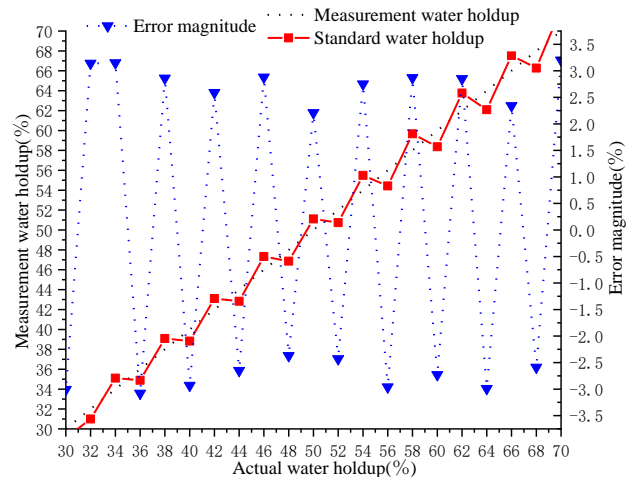


Fig. 8. Experimental chart of random measurement of the oil-water two-phase flow holdup

From the above analysis, the repeatability of the flow rate is less than 0.0002 and the repeatability of the holdup is 0.0003. Therefore, the measurement results have high repeatability.

The prototype designed in this paper can measure high water holdup and low flow rate of oil-water two-phase flow. If the liquid level at the conductance sensor is smooth, the volume of the prototype does not need to be increased when the flow rate increases. Otherwise, the volume of the prototype must be increased.

6. CONCLUSIONS

A flow rate and holdup measurement method of oil-water two-phase flow based on phase state regulation is proposed. This method does not depend on sensor accuracy and reduces sensor accuracy requirements. The volume of the experimental prototype based on this method is small and overcomes the disadvantage of too large volume of the separation method. The conclusions are as follows:

1. The phase state regulation of oil-water two-phase flow is proposed, which regulates the mixed oil-water two-phase flow into single-phase water flow and single-phase oil flow.
2. The wavelet analysis method for detecting the oil-water two-phase flow phase change point is proposed, which can effectively detect the phase change point.
3. Through simulation, the prototype parameters are determined and a flow rate and holdup measurement experiments are performed. The experiment results show that the water measurement accuracy of flow rate is better than 3.73%, the oil measurement accuracy of the holdup is better than 3.68% and the maximum measurement error of holdup is 3.23%. The repeatability of the flow rate is less than 0.0002 and the repeatability of the holdup is 0.0003.

ACKNOWLEDGMENT

This work is partially supported by the National Natural Science Foundation of China (51774092, 52174021), National Natural Science Foundation of Heilongjiang Province (LH2020E012), Blue Project of Universities in Jiangsu Province of China (202201022) and Industry Foresight and Key Technology Projects of Suzhou of China (SYC2022149).

REFERENCES

- [1] Han, L. F., Wang, H. X., Cong, Y., Liu, X. B., Han, J., Fu, C. F. (2020). Oil phase velocity measurement of oil-water two-phase flow with low velocity and high water cut using the improved ORB and RANSAC algorithm. *Measurement Science Review*, 20 (2), 93-103. <https://doi.org/10.2478/msr-2020-0012>
- [2] Li, Z. C., Fan, C. L. (2020). A novel method to identify the flow pattern of oil-water two-phase flow. *Journal of Petroleum Exploration and Production Technology*, 10 (8), 3723-3732. <https://doi.org/10.1007/s13202-020-00987-1>
- [3] Karimi, M. A., Arsalan, M., Shamim, A. (2016). Low cost and pipe conformable microwave-based water-cut sensor. *IEEE Sensors Journal*, 16 (21), 7636-7645. <https://doi.org/10.1109/JSEN.2016.2599644>
- [4] Wu, H., Tan, C., Dong, X. X., Dong, F. (2015). Design of a conductance and capacitance combination sensor for water holdup measurement in oil-water two-phase flow. *Flow Measurement and Instrumentation*, 46, 218229. <https://doi.org/10.1016/j.flowmeasinst.2015.06.026>
- [5] Liu, D. X., Liu, L., Bai, D. F., Diao, Y. L. (2023). Experimental study of loss coefficients for laminar oil-water two-phase flow through micro-scale flow restrictions. *Experimental Thermal and Fluid Science*, 140, 110747. <https://doi.org/10.1016/j.expthermflusci.2022.110747>
- [6] Men, X. Y., Yan, X., Chen, Y. C., Li, Z. B., Gong, H. J. (2017). Gas-water phase flow production stratified logging technology of coalbed methane wells. *Petroleum Exploration and Development*, 44 (2), 315-320. [https://doi.org/10.1016/S1876-3804\(17\)30036-8](https://doi.org/10.1016/S1876-3804(17)30036-8)
- [7] Dzemic, Z., Sirok, B., Bizjan, B. (2018). Turbine flowmeter response to transitional flow regimes. *Flow Measurement and Instrumentation*, 59, 18-22. <https://doi.org/10.1016/j.flowmeasinst.2017.11.006>
- [8] Chen, J. H., Anastasiou, C., Chen, S. B., Basha, N. M., Kahouadji, L., Arcucci, R., Angeli, P., Matar, O. K. (2023). Computational fluid dynamics simulations of phase separation in dispersed oil-water pipe flows. *Chemical Engineering Science*, 267, 239-248. <https://doi.org/10.1016/j.ces.2022.118310>
- [9] Dayev, Z. A. (2022). General theory of invariant methods for measuring the flow rate of multicomponent flows. *Flow Measurement and Instrumentation*, 85, 102145. <https://doi.org/10.1016/j.flowmeasinst.2022.102145>
- [10] Huang, J. C., Sheng, B. X., Ji, H. F., Huang, Z. Y., Wang, B. L., Li, H. Q. (2019). A new contactless bubble/slug velocity measurement method of gas-liquid two-phase flow in small channels. *IEEE Transactions on Instrumentation and Measurement*, 68 (9), 3253-3267. <https://doi.org/10.1109/TIM.2018.2877825>
- [11] Karimi, M. A., Arsalan, M., Shamim, A. (2021). Extended throat venturi based flow meter for optimization of oil production process. *IEEE Sensors Journal*, 21 (16), 17808-17816. <https://doi.org/10.1109/JSEN.2021.3083532>
- [12] Kang, W., Lee, S. H., Lee, S. J., Ha, Y. C., Jung, S. S. (2018). Effect of ultrasonic noise generated by pressure control valves on ultrasonic gas flowmeters. *Flow Measurement and Instrumentation*, 60, 95-104. <https://doi.org/10.1016/j.flowmeasinst.2018.02.023>
- [13] Liang, G. H., Ren, S. J., Dong, F. (2020). An inclusion boundary and conductivity simultaneous estimation method for ultrasound reflection guided electrical impedance tomography. *IEEE Sensors Journal*, 20 (19), 11578-11587. <https://doi.org/10.1109/JSEN.2020.2998852>
- [14] Zhao, N., Wang, Y. J., Liu, X. B. (2011). The research of measuring method by thermal trace correlation in the horizontal well. *Petroleum Instruments*, 25, 57-59. <https://doi.org/10.3969/j.issn.1004-9134.2011.02.021>
- [15] Lin, D., Grundmann, J., Eltner, A. (2019). Evaluating image tracking approaches for surface velocimetry with thermal tracers. *Water Resources Research*, 55 (4), 3122-3136. <https://doi.org/10.1029/2018WR024507>
- [16] Yang, H. Y., Qing, G. M., Chen, Y., Zhao, H. (2020). Optimization of coil width and magnetic field switching speed for non-contacted electromagnetic flowmeter. *IEEE Sensors Journal*, 20 (10), 5329-5335. <https://doi.org/10.1109/JSEN.2020.2969211>
- [17] Gao, S., Ma, H. (2022). A study on structure improvement scheme of electromagnetic flow sensor for slurry flow measurement. *Measurement & Control*, 55 (5-6), 519-534. <https://doi.org/10.1177/00202940211064589>

- [18] Sharma, P., Lao, L., Falcone, G. (2018). A microwave cavity resonator sensor for water-in-oil measurements. *Sensors and Actuators B: Chemical*, 202, 200-210. <https://doi.org/10.1016/j.snb.2018.01.211>
- [19] Karimi, M. A., Arsalan, M., Shamim, A. (2017). A low-cost, orientation-insensitive microwave water-cut sensor printed on a pipe surface. In *2017 IEEE MTT-S International Microwave Symposium (IMS)*. IEEE, 1218-1221. <https://doi.org/10.1109/MWSYM.2017.8058822>
- [20] Guo, S. N., Sun, L. J., Zhang, T., Yang, W. L., Yang, Z. (2013). Analysis of viscosity effect on turbine flowmeter performance based on experiments and CFD simulations. *Flow Measurement and Instrumentation*, 34 (5), 42-52. <https://doi.org/10.1016/j.flowmeasinst.2013.07.016>
- [21] Zhu, K., Chen, X. Y., Qu, M. G., Yang, D. F., Hu, L., Xu, J. H., Xie, J. (2020). An ultrasonic flowmeter for liquid flow measurement in small pipes using AlN piezoelectric micromachined ultrasonic transducer arrays. *Journal of Micromechanics and Microengineering*, 30 (12), 125010. <https://doi.org/10.1088/1361-6439/abc100>
- [22] Zhai, L. S., Zhang, H. X., Jin, N. D. (2020). Prediction of pressure drop for segregated oil-water flows in small diameter pipe using modified two-fluid model. *Experimental Thermal and Fluid Science*, 114, 110078. <https://doi.org/10.1016/j.expthermflusci.2020.110078>
- [23] Han, L. F., Hou, Y. D., Wang, Y. J., Liu, X. B., Han, J., Xie, R. H., Mu, H. W., Fu, C. F. (2019). Measurement of velocity of sand-containing oil-water two-phase flow with super high water holdup in horizontal small pipe based on thermal tracers. *Flow Measurement and Instrumentation*, 69, 101622. <https://doi.org/10.1016/j.flowmeasinst.2019.101622>
- [24] Casacuberta, N., Smith, J. N. (2012). Nuclear reprocessing tracers illuminate flow features and connectivity between the arctic and subpolar north atlantic oceans. *Annual Review of Marine Science*, 428, 182-190. <https://doi.org/10.1146/annurev-marine-032122-112413>
- [25] Yadav, A., Pant, H. J., Roy, S. (2020). Velocity measurements in convective boiling flow using radioactive particle tracking technique. *Aiche Journal*, 66 (1), 16782. <https://doi.org/10.1002/aic.16782>
- [26] Kohli, M. A., Schmoldt, J. P. (2022). Feasibility of UXO detection via pulsed neutron-neutron logging. *Applied Radiation and Isotopes*, 188, 110403. <https://doi.org/10.1016/j.apradiso.2022.110403>
- [27] Wang, X. G., Zhang, F., Ma, H. Y., Zhou, L. W. (2021). A novel borehole/annulus holdup calculation method based on pulsed neutron logging. *Applied Radiation and Isotopes*, 168, 109479. <https://doi.org/10.1016/j.apradiso.2020.109479>
- [28] Jin, N. D., Yu, C., Han, Y. F., Yang, Q. Y., Ren, Y. Y., Zhai, L. S. (2021). The performance characteristics of electromagnetic flowmeter in vertical low-velocity oil-water two-phase flow. *IEEE Sensors Journal*, 21 (1), 464-475. <https://doi.org/10.1109/JSEN.2020.3013327>
- [29] Perera, K., Time, R. W., Pradeep, C., Kumara, A. S. (2021). Interfacial wave analysis of low viscous oil-water flow in upwardly inclined pipes. *Chemical Engineering Science*, 196, 444-462. <https://doi.org/10.1016/j.ces.2018.11.014>
- [30] Huang, L., Deng, S., Chen, M., Guan, J. F. (2017). Numerical simulation and experimental study on a deoiling rotary hydrocyclone. *Chemical Engineering Science*, 172, 107-116. <https://doi.org/10.1016/j.ces.2017.06.030m>
- [31] Liu, L., Zhao, L. X., Yang, X., Wang, W. H., Xu, B. R., Liang, B. (2019). Innovative design and study of an oil-water coupling separation magnetic hydrocyclone. *Separation and Purification Technology*, 213, 389-400. <https://doi.org/10.1016/j.seppur.2018.12.051>
- [32] Li, S., Li, R. N., Wang, Z. C., Xu, D. K., Yan, Y. J., Xu, Y., Li, J. S., Chen, X. (2019). Fluid-structure interaction vibration response analysis of the hydrocyclone under periodic excitation. *IEEE Access*, 7, 146273-146281. <https://doi.org/10.1109/ACCESS.2019.2945837>

Received February 02, 2023

Accepted October 20, 2023